

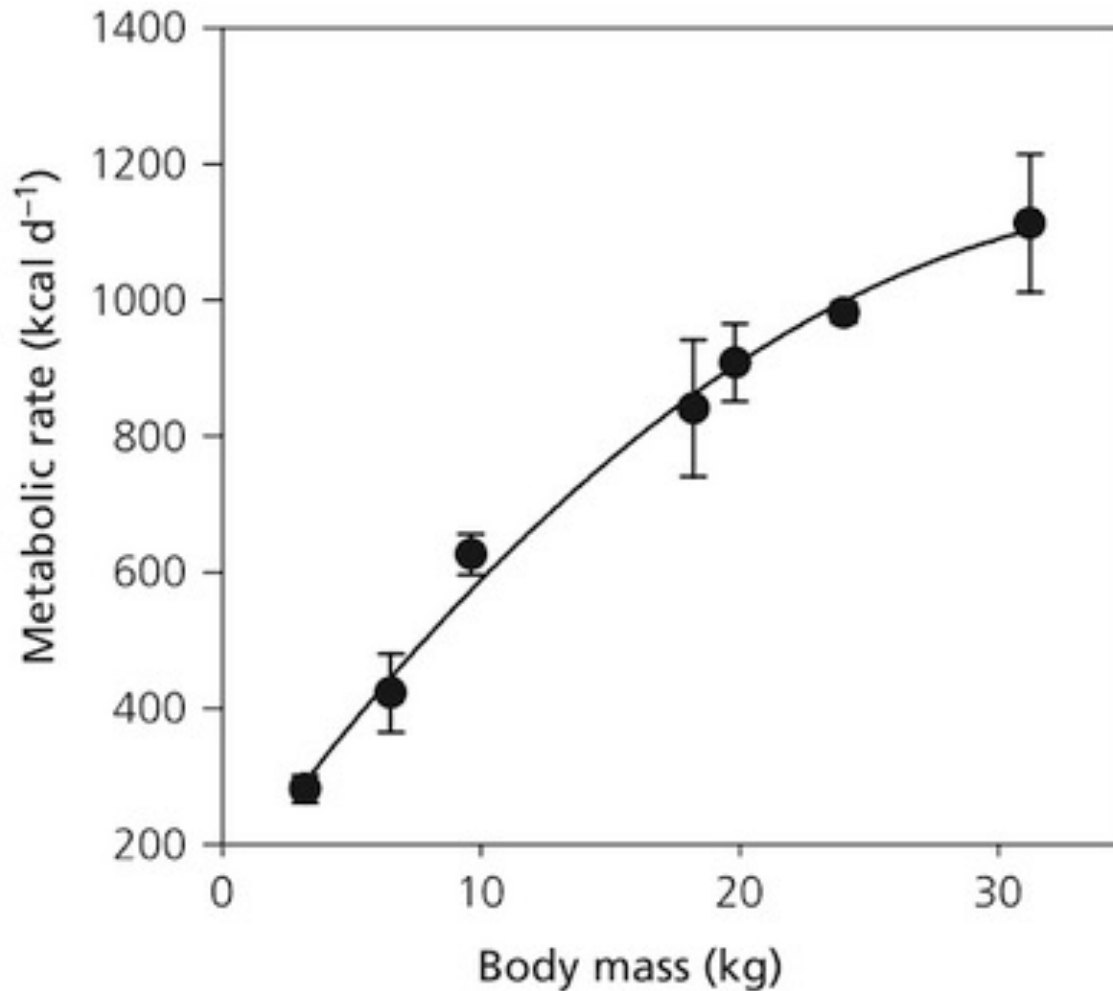
Metabolic Theory of Ecology, size spectra and ecological pyramids

Four things you need to know about metabolism and community ecology

1. (Field) metabolic rates scale in a fairly predictable manner with body size, $b \sim 0.75$ i.e. $3/4$, due to architecture of vascular network that supplies oxygen & nutrients (West, Brown, Enquist, WBE)
2. Organismal metabolic rates are not as high as they could be, especially for larger animals. Metabolic rate is limited by the network-limiting rate of flow of respiratory substrates (food, O_2) from the outside to the mitochondria
3. Temperature & metabolism; Q_{10} s & Boltzmann-Arrhenius
4. Metabolism explains and underpins some profound scaling patterns in ecology, inc. community ecology, such as size spectra & ecological pyramids

Metabolism in Domestic Dogs

Max Rubner (1883)



Determining the scaling exponent

Julian Huxley described the change in size of organism features with body size using a power law

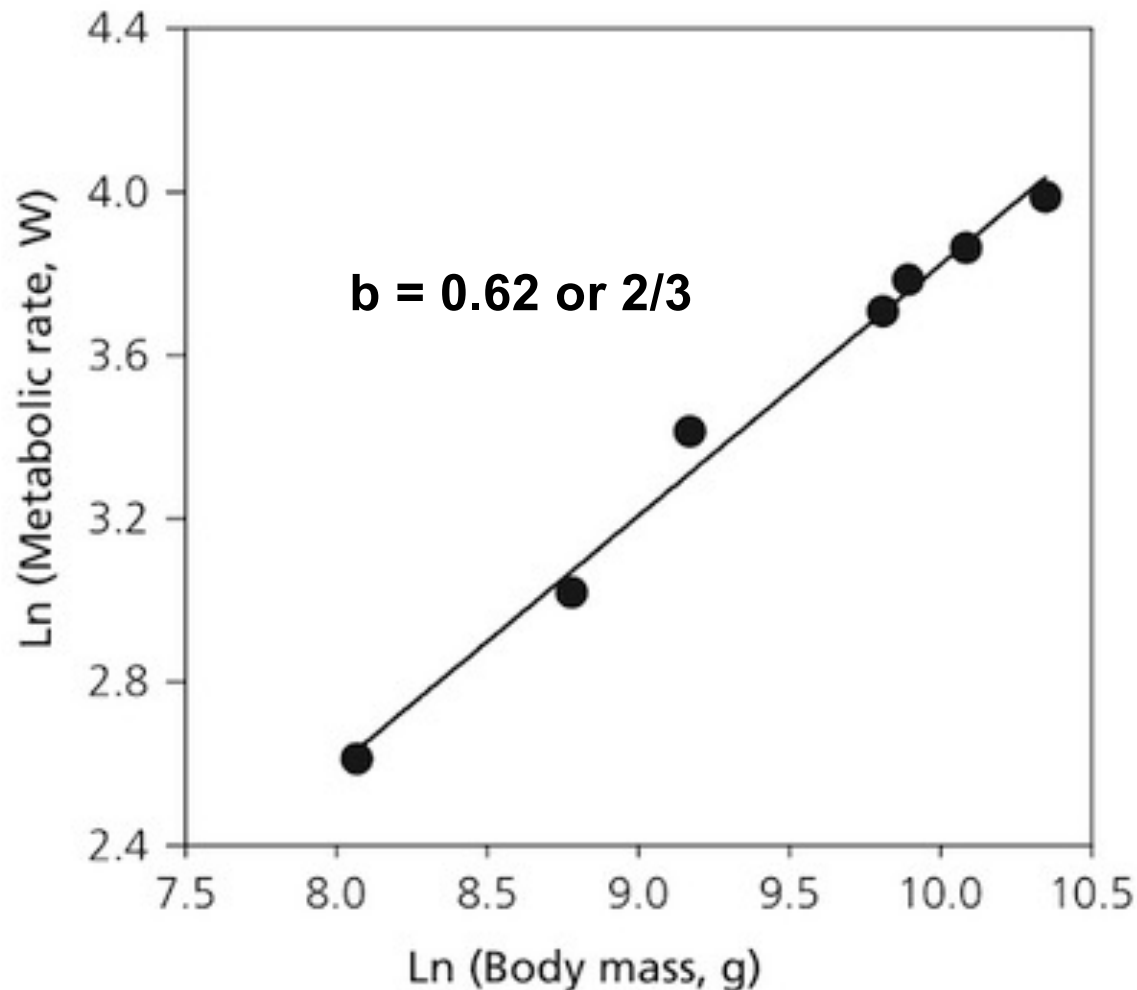
$Y = aM^b$, a = constant, b is scaling exponents

This can be linearised by logging it

$$\ln(Y) = \ln(a) + b\ln(M)$$

Metabolism in Domestic Dogs

Max Rubner (1883) revisited



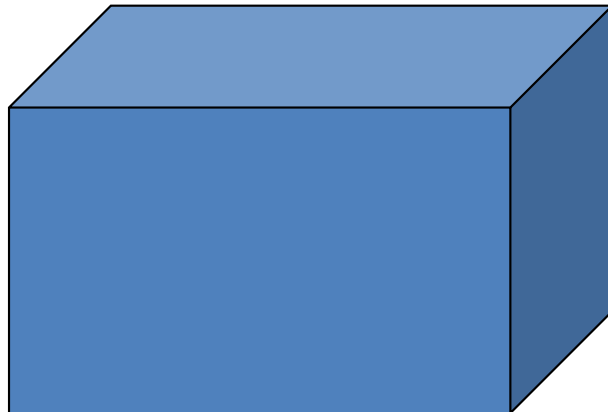
Watts = SI unit of 1 joule per second (vs. Kcal per day)

Surface area to volume ratio leads to
the expectation $B \sim \text{Mass}^{2/3}$
[square cube law]

Length = x

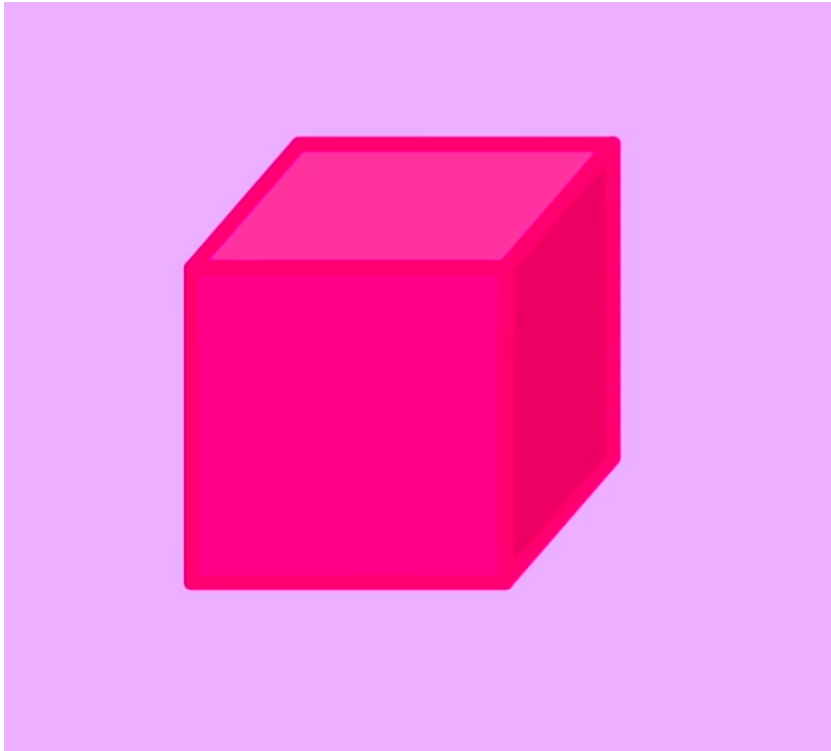


Surface area = x^2

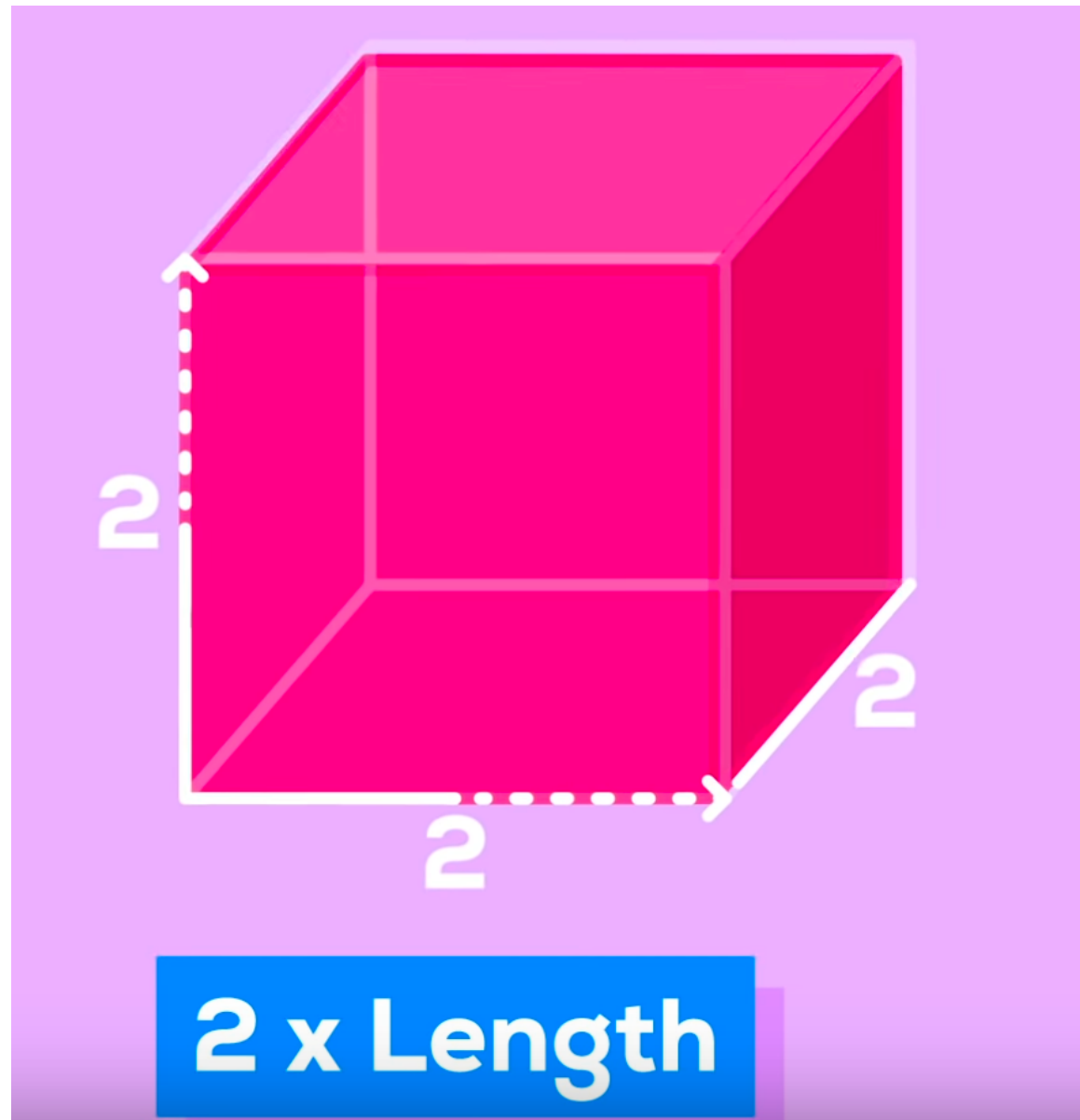


Volume = x^3

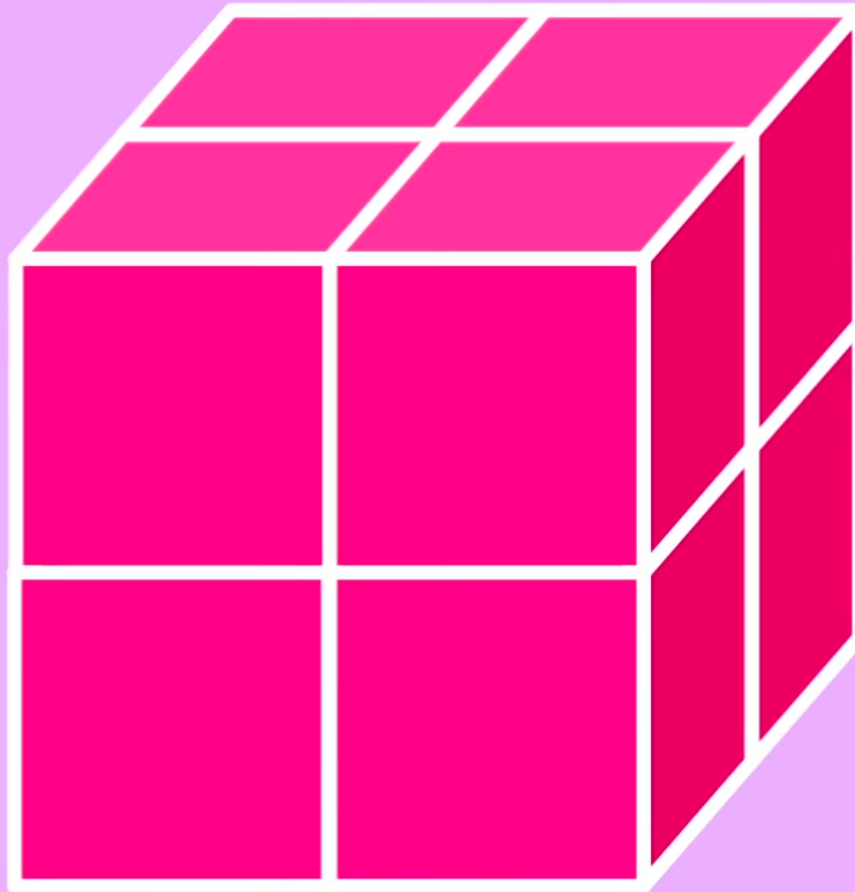
Square cube law



When doubling the length of a side, surface and volume do not double

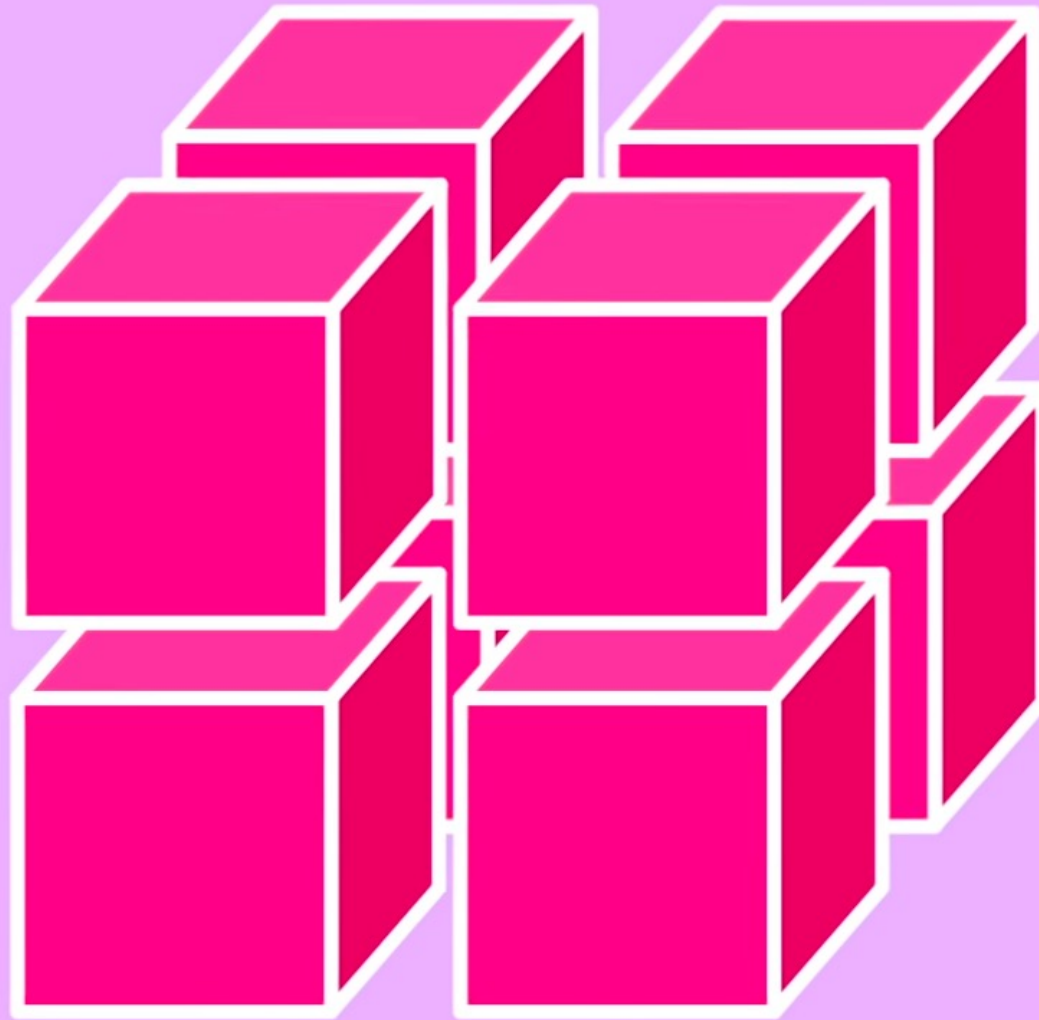


4x surface area



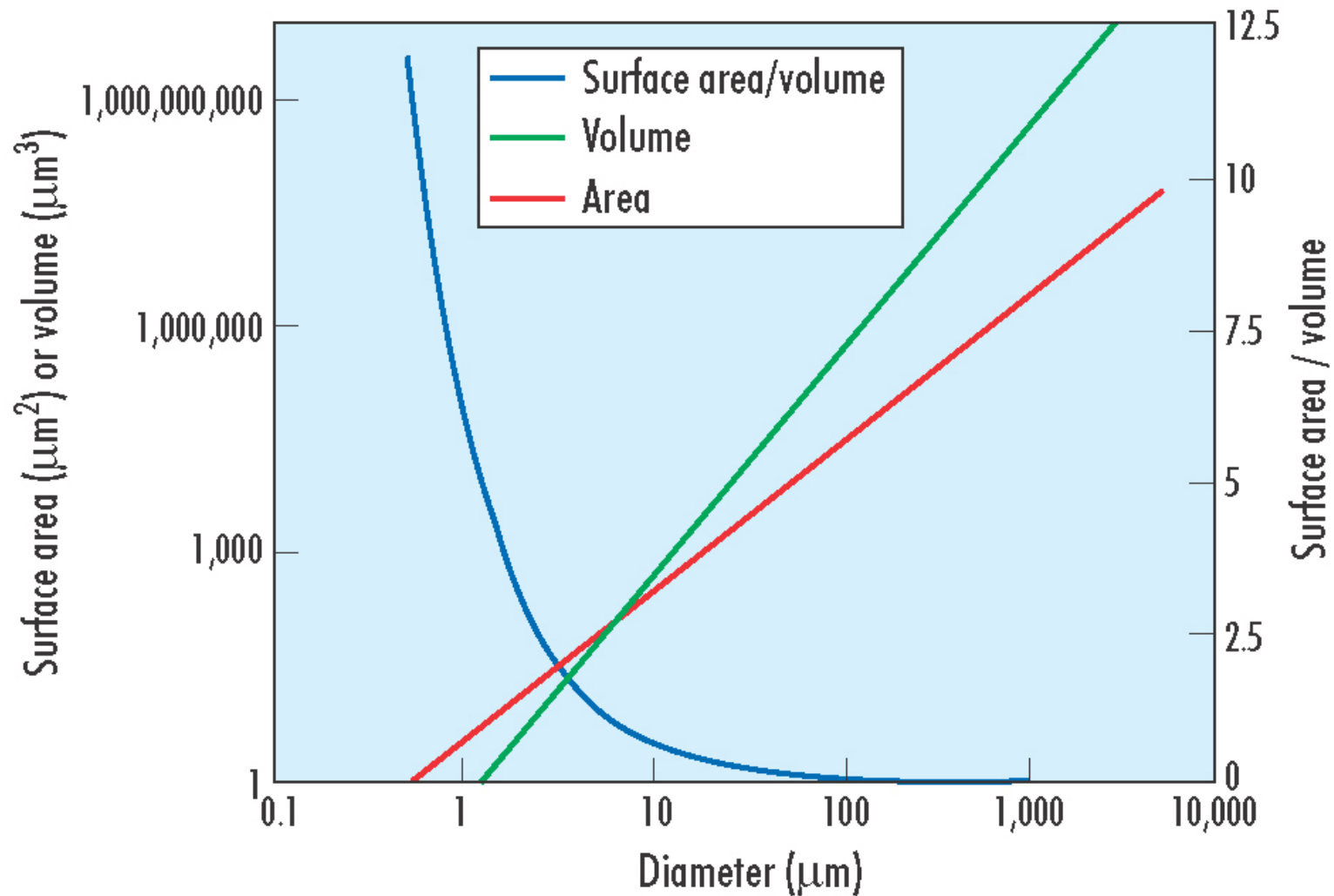
$$1 \text{ cm}^2 \rightarrow 4 \text{ cm}^2$$

8x the volume



$$1 \text{ cm}^3 \rightarrow 8 \text{ cm}^3$$

Null geometric expectations



This is the basis for the Gill Oxygen Limitation Theory of Daniel Pauly

Kleiber's law

But metabolic rate (B) scales with body mass (M) to the power of $\frac{3}{4}$ NOT $\frac{2}{3}$, $B = M^{3/4}$

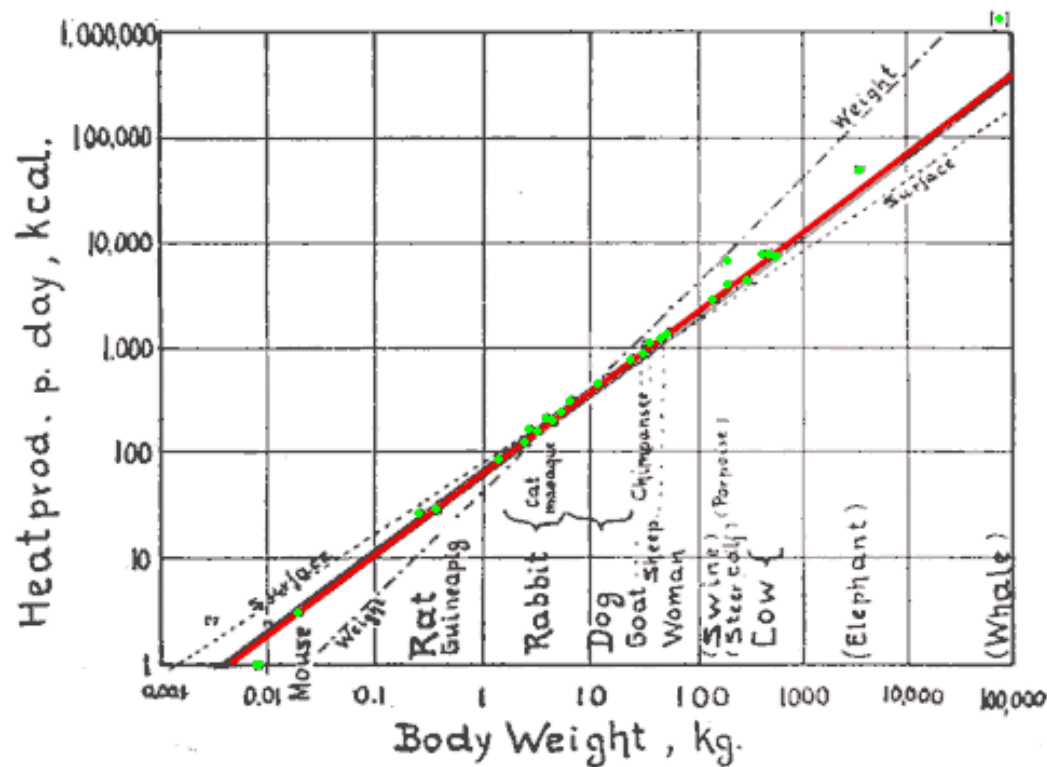
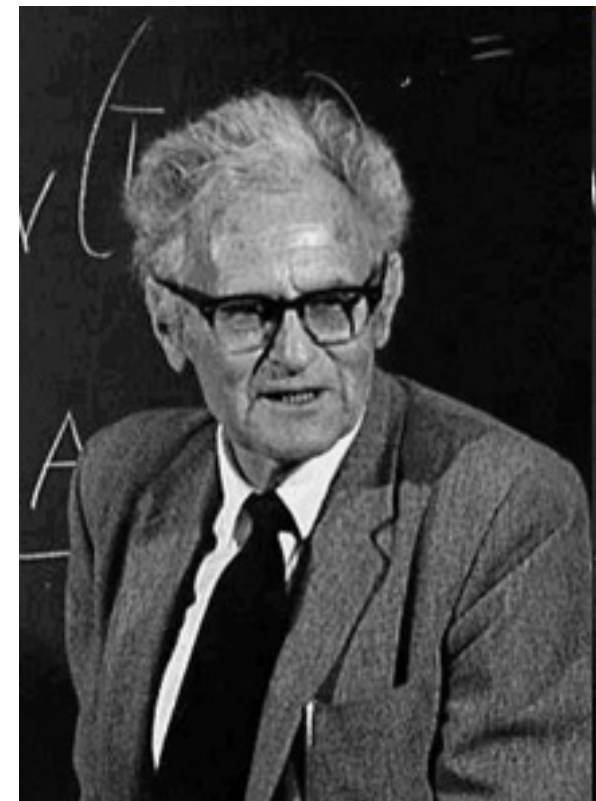
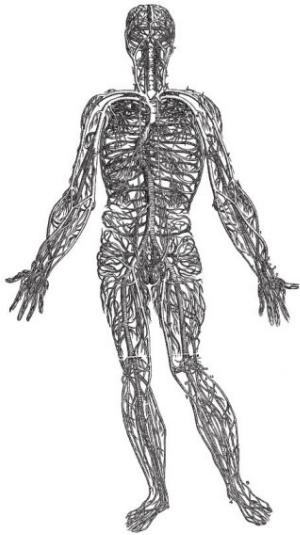


Fig. 1. Log. metabol. rate/log body weight



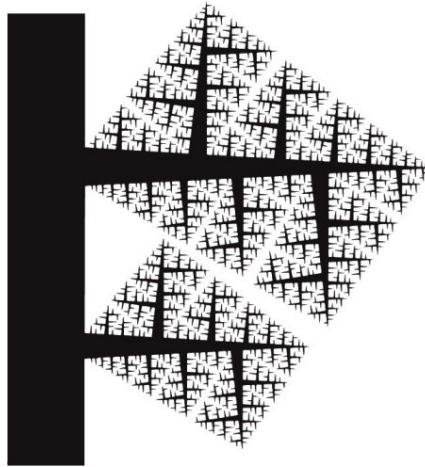
We are not three-dimensional spheres – the 4th dimension is inside

(a) Fractal theory



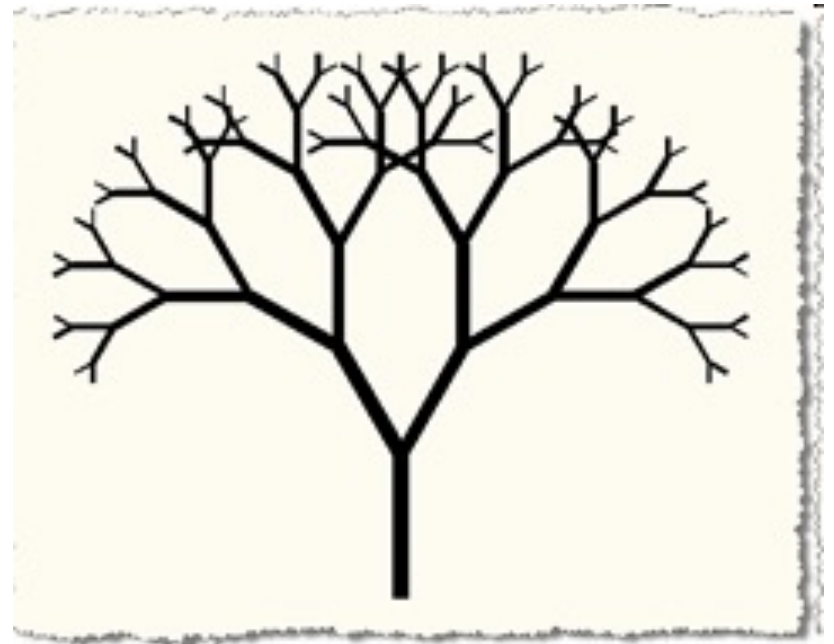
Vesalius 1543: One of the first anatomically accurate images of the human circulatory system

Animal Physiology 2e, Figure 6.13 (Part 1)



Mandelbrot 1983: A fractal model of a branching system such as the circulatory system

© 2008 Sinauer Associates, Inc.



The 4th dimension is the fractal distribution networks inside our body

(Three-) Quarter power scaling appears when

Space-filling networks service all
locally biologically active regions

The terminal units of networks
are invariant within a class or
taxon (respiratory complex
enzymes == water taps)

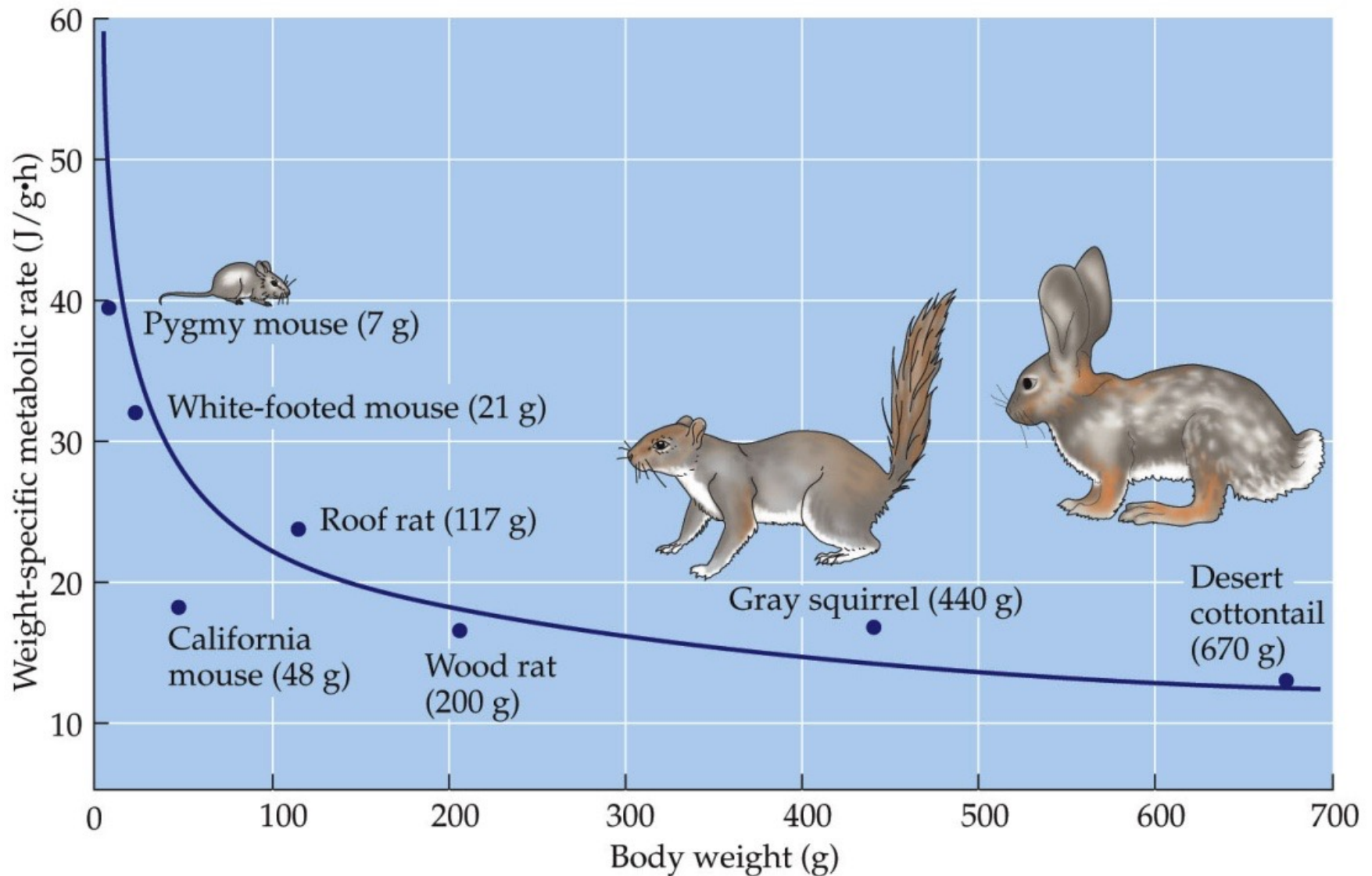
Evolution toward minimisation of
energy costs of resource
distribution



West, G. B., Brown, J. H., and Enquist, B. J. (1997). A general model for the origin of allometric scaling laws in biology. *Science* 276, 122-126.

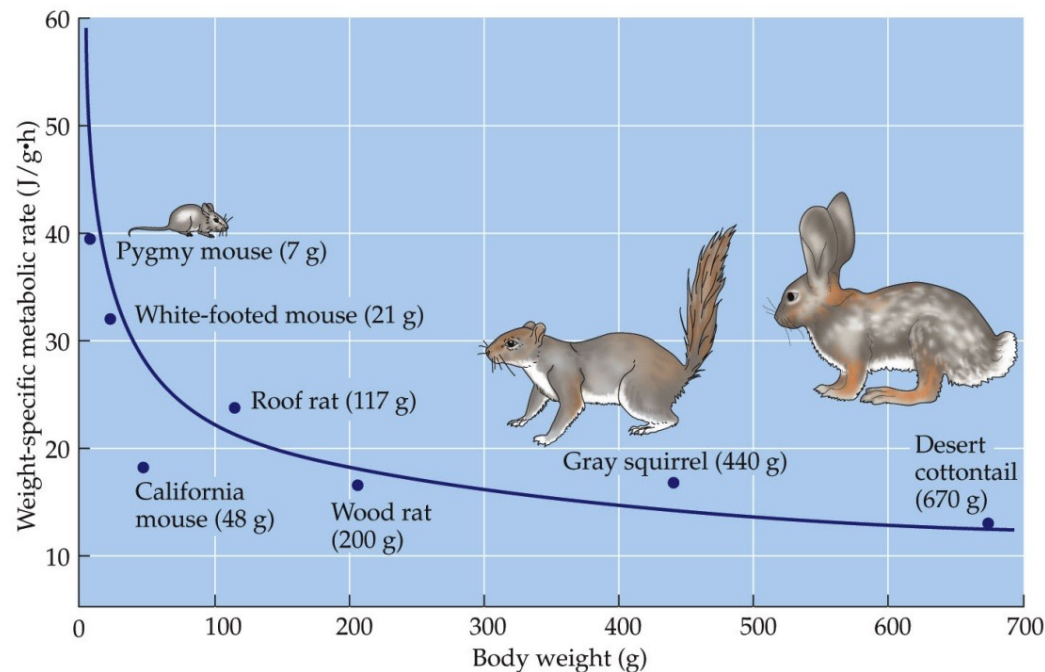
West, G. B., Brown, J. H., and Enquist, B. J. (1999). The fourth dimension of life: Fractal geometry and allometric scaling of organisms. *Science* 284, 1677-1679.

Beware of Y-axis when...



...moving btw individual (3/4) and mass-specific (-1/4) metabolic rate

1. $W = M^{3/4}$ (whole organism metabolic rate)
2. $\text{Mass} = M^1$
3. I, individual mass specific rates (per gram) =
 $M^{3/4} / M^1 = M^{0.75-1} = M^{-1/4}$ or -0.25



Animal Physiology 2e, Figure 6.8

© 2008 Sinauer Associates, Inc.

Heart rate scales across organisms to $M^{-1/4}$

Values of allometric exponents for variables of the mammalian cardiovascular and respiratory systems predicted by the fractal model compared with empirical observations

Table 1. Values of allometric exponents for variables of the mammalian cardiovascular and respiratory systems predicted by the model compared with empirical observations. Observed values of exponents are taken from (2, 3); ND denotes that no data are available.

Cardiovascular			Respiratory		
Variable	Exponent		Variable	Exponent	
	Predicted	Observed		Predicted	Observed
Aorta radius r_0	$3/8 = 0.375$	0.36	Tracheal radius	$3/8 = 0.375$	0.39
Aorta pressure Δp_0	$0 = 0.00$	0.032	Interpleural pressure	$0 = 0.00$	0.004
Aorta blood velocity u_0	$0 = 0.00$	0.07	Air velocity in trachea	$0 = 0.00$	0.02
Blood volume V_b	$1 = 1.00$	1.00	Lung volume	$1 = 1.00$	1.05
Circulation time	$1/4 = 0.25$	0.25	Volume flow to lung	$3/4 = 0.75$	0.80
Circulation distance l	$1/4 = 0.25$	ND	Volume of alveolus V_A	$1/4 = 0.25$	ND
Cardiac stroke volume	$1 = 1.00$	1.03	Tidal volume	$1 = 1.00$	1.041
Cardiac frequency ω	$-1/4 = -0.25$	-0.25	Respiratory frequency	$-1/4 = -0.25$	-0.26
Cardiac output \dot{E}	$3/4 = 0.75$	0.74	Power dissipated	$3/4 = 0.75$	0.78
Number of capillaries N_c	$3/4 = 0.75$	ND	Number of alveoli N_A	$3/4 = 0.75$	ND
Service volume radius	$1/12 = 0.083$	ND	Radius of alveolus r_A	$1/12 = 0.083$	0.13
Womersley number α	$1/4 = 0.25$	0.25	Area of alveolus A_A	$1/6 = 0.083$	ND
Density of capillaries	$-1/12 = -0.083$	-0.095	Area of lung A_L	$11/12 = 0.92$	0.95
O ₂ affinity of blood P_{50}	$-1/12 = -0.083$	-0.089	O ₂ diffusing capacity	$1 = 1.00$	0.99
Total resistance Z	$-3/4 = -0.75$	-0.76	Total resistance	$-3/4 = -0.75$	-0.70
Metabolic rate B	$3/4 = 0.75$	0.75	O ₂ consumption rate	$3/4 = 0.75$	0.76

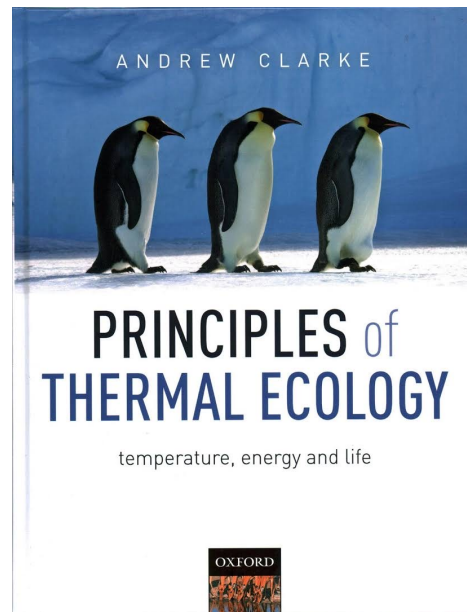
Four things you need to know about life histories and metabolism

1. (Field) metabolic rates scale in a fairly predictable manner with body size, $b \sim 0.8 \sim 3/4$, due to architecture of vascular network that supplies oxygen & nutrients (West, Brown, Enquist)
2. Metabolic rates are not as high as they could be, especially for larger animals. Metabolic rate is limited by the network-limiting rate of flow of respiratory substrates (food, O_2) from the outside to the mitochondria
3. Temperature & metabolism; Q10s & Boltzmann-Arrhenius
4. Metabolism explains and underpins some profound scaling patterns in ecology, inc. community ecology, such as size spectra.

Clarke's paradox

Does the metabolic rate of the cell determine the rate at which nutrients must be supplied or...

... Is the metabolic rate of a cell determined by the rate of nutrient/oxygen supply (WBE)?



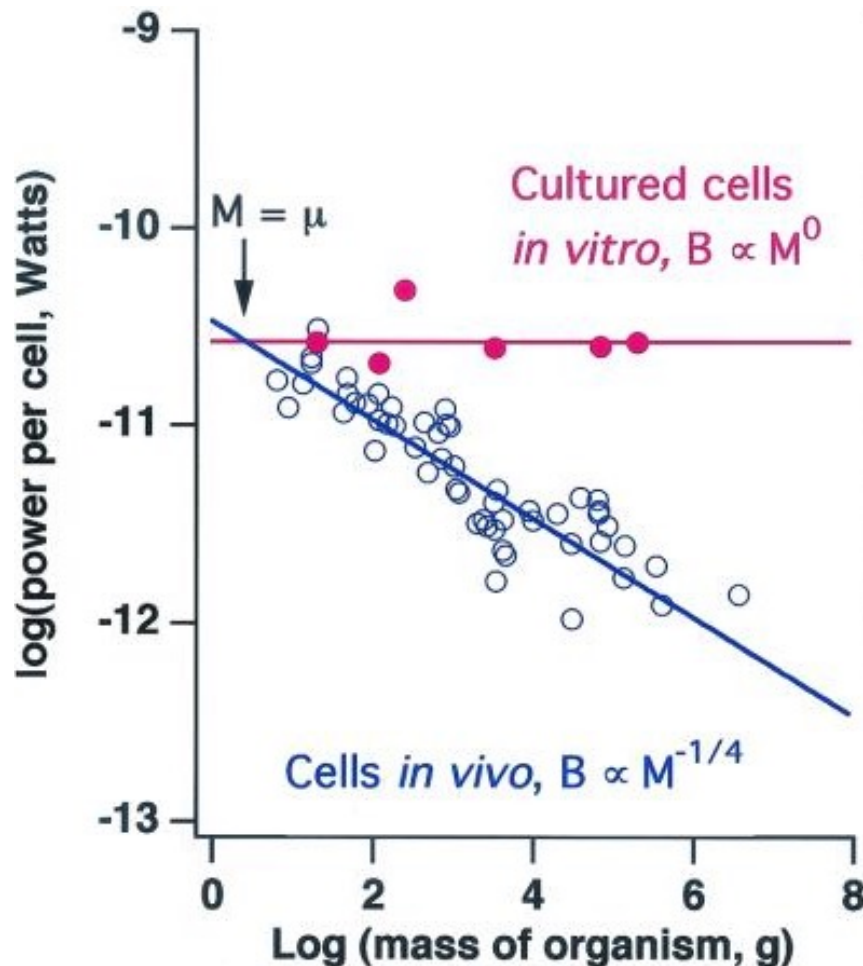
If classic metabolic physiology is correct, then cells power should vary with size and cells of larger animals should have lower power....

If West, Brown, Enquist are right then individual animal cells should have the same power

But only when removed from the constraint of the fractal supply of materials

No $\frac{1}{4}$ scaling when cells are removed from supply limits of fractal network

Cells removed from the body and cultured *in vitro* take on a constant metabolic rate

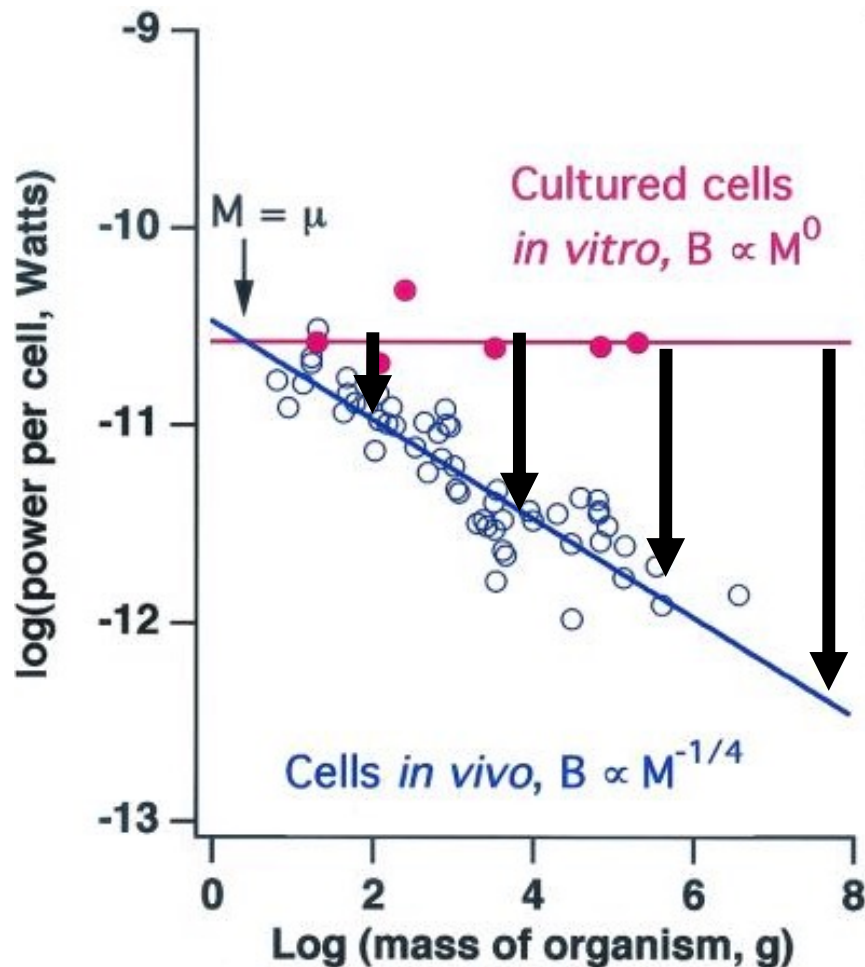


West, G. B., Woodruff, W. H., and Brown, J. H. (2002). Allometric Scaling of Metabolic Rate from Molecules and Mitochondria to Cells and Mammals. *Proceedings Of the National Academy Of Sciences Of the United States Of America* 99, 2473-2478.



Fig. 2. Metabolic power of single mammalian cells as a function of body mass on a logarithmic scale. Blue circles represent cells *in vivo* calculated for the same mammals as described in Fig. 1. Red circles represent cultured cells *in vitro* of six mammalian species: mouse, hamster, rat, rhesus monkey, human, and pig (32). The solid blue line is the $M^{-1/4}$ prediction for cells *in vivo* from Eq. 3, and the solid red line is the predicted constant for cells *in vitro* from Eq. 5. The two lines are predicted to intersect at $M = \mu \approx 1$ g, at which they have the value $B \approx 3 \times 10^{-11}$ W.

No fractal network – no $\frac{1}{4}$ scaling



Cells removed from the body and cultured *in vitro* take on a constant metabolic rate

Depression in power output because of limited input

Four things you need to know about life histories and metabolism

1. (Field) metabolic rates scale in a fairly predictable manner with body size, $b \sim 0.8 \sim 3/4$, due to architecture of vascular network that supplies oxygen & nutrients (West, Brown, Enquist)
2. Metabolic rates are not as high as they could be, especially for larger animals. Metabolic rate is limited by the network-limiting rate of flow of respiratory substrates (food, O_2) from the outside to the mitochondria
3. **Temperature & metabolism; Q_{10} s & Boltzmann-Arrhenius**
4. Metabolism explains and underpins some profound scaling patterns in ecology, inc. community ecology, such as size spectra.

Back to temperature scaling & MTE

Standard formulation is Q_{10}

$$Q_{10} = \left(\frac{R_2}{R_1} \right)^{\left(\frac{10}{T_2 - T_1} \right)}$$

Rates double over a 10-degree temperature rise

This is a linear approximation to the process below.

$$B = b_0 M^{3/4} e^{-E/kt},$$

where

b_0 = normalisation constant (intercept)

M = body mass

$e^{-E/kt}$ = Boltzmann-Arrhenius term

$$e^{-E/kt} = \text{Boltzmann-Arrhenius term}$$

The Boltzmann-Arrhenius term characterises the exponential effects of temperature (t in Kelvin [$^{\circ}\text{C} + 273.15$]), where:

E is average activation energy of the respiratory complex
 ~ 0.65 eV for animals

k is Boltzmann's constant 8.62×10^{-5} eV K^{-1}

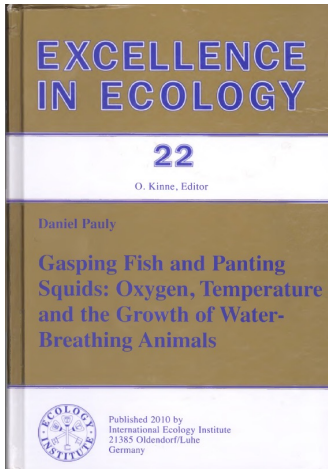
$1\text{eV} = 23.06 \text{ kcal/mol} = 96.49 \text{ kJ/mol}$

(Easy to find on wikipedia)

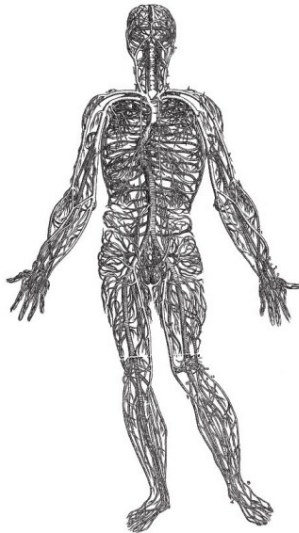
Current controversies & MTE

- New more refined analyses of Basal MR and Field MR reveal that smaller animals scale $M^{2/3}$ and larger ones $M^{3/4}$
- Boltzmann-Arrhenius based on reactions in gas phase
- The B-A model is consistent with Q10s, (the increases in rate for a 10°C T increase.
- The MTE has only vessels and enzymes, there is no heart nor a consideration of respiratory surface area, room for Pauly's Gill-Oxygen Limitation Theory

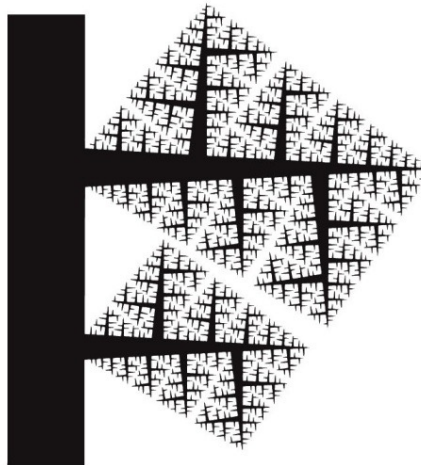
MTE has circulation but where's the respiration?



(a) Fractal theory



Vesalius 1543: One of the first anatomically accurate images of the human circulatory system



Mandelbrot 1983: A fractal model of a branching system such as the circulatory system

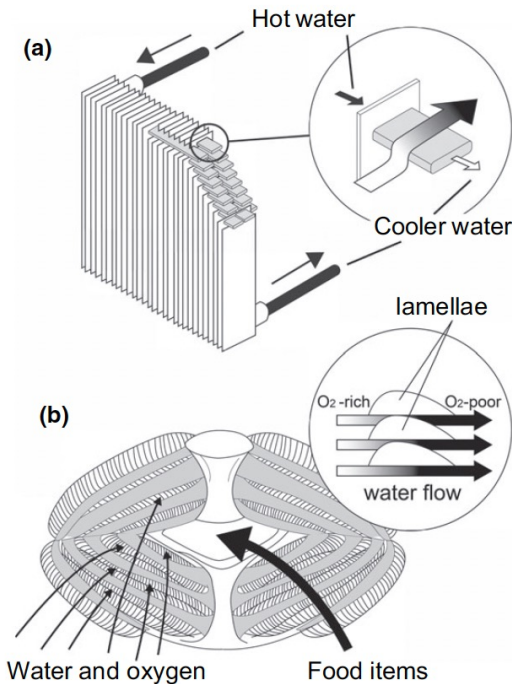


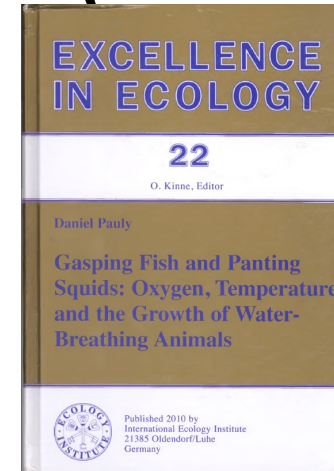
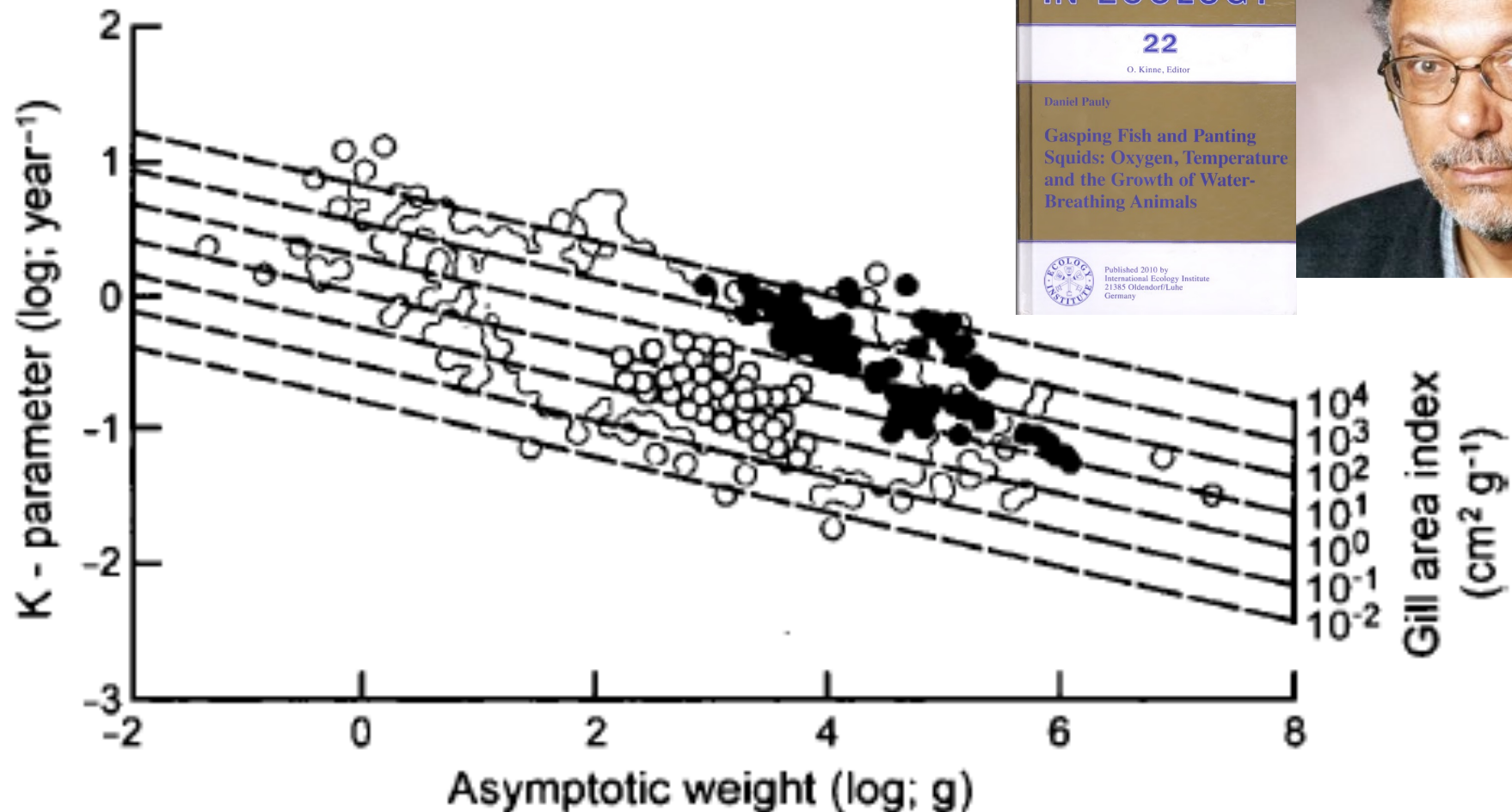
FIGURE 1 Illustrating the similarity between systems for cooling car engines and for extracting oxygen from water. (a) Schematic representation of a car's radiator, which can grow in width and height, but not in depth, as air, once it has passed by a first row of lamellae (insert), cannot pick up more heat. (b) Frontal view of the interior of a manta's mouth (*Mobula japonica*; adapted from Figure 3.20A of Wegner (2015)), illustrating the two dimensionality of breathing, that is, the fact that once water has passed through the gills (insert), it has become depleted of oxygen, and it would be useless for it to pass through more gill structure

Animal Physiology 2e, Figure 6.13 (Part 1)

© 2008 Sinauer Associates, Inc.

Pauly D. 1981. The relationships between gill surface area and growth performance in fish: a generalisation of von Bertalanffy's theory of growth. *Meeresforschung* 28: 251-282.

Gill area index explains growth performance in fishes (k & W_{∞})



Pauly D. 1981. The relationships between gill surface area and growth performance in fish: a generalisation of von Bertalanffy's theory of growth. *Meeresforschung* 28: 251-282.

Respiratory surface area twice as important as temperature for explaining variance in vertebrate MR

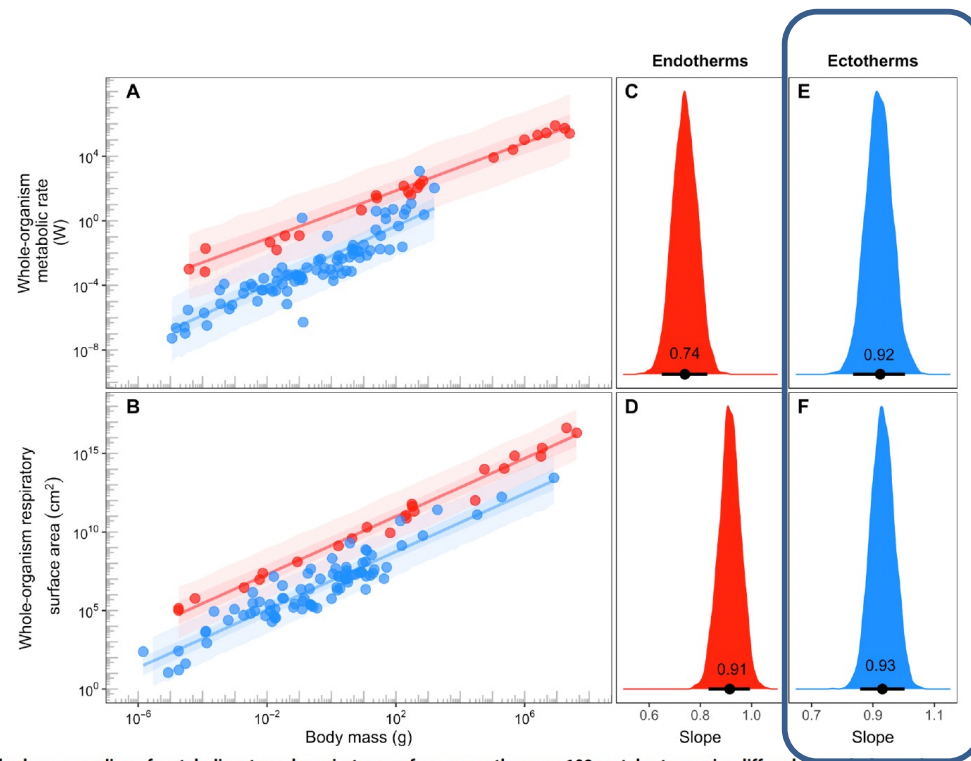


Fig. 4. The body mass scaling of metabolic rate and respiratory surface across the same 109 vertebrate species differed for endotherms but was similar for ectotherms. While (whole-organism) metabolic rate body mass scaling exponents (i.e., allometric slopes) differed between endotherms and ectotherms (A, C, and

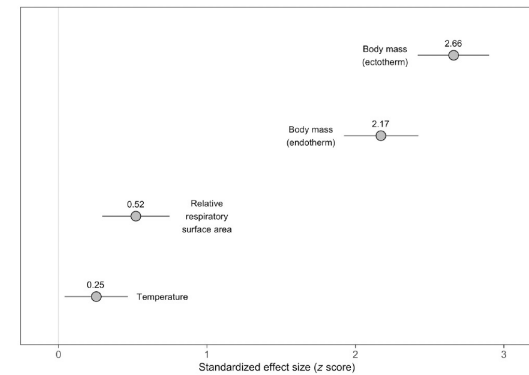


Fig. 3. Compared to temperature, respiratory surface area explains twice as much variation in metabolic rate across the vertebrate tree of life. The mean (gray

Bigman et al. (2021). Respiratory capacity is twice as important as temperature in driving patterns of metabolic rate across the vertebrate tree of life. *Science Advances*, 7, eabe5163.

Four things you need to know about life histories and metabolism

1. (Field) metabolic rates scale in a fairly predictable manner with body size, $b \sim 0.8 \sim 3/4$, due to architecture of vascular network that supplies oxygen & nutrients (West, Brown, Enquist)
2. Metabolic rates are not as high as they could be, especially for larger animals. Metabolic rate is limited by the network-limiting rate of flow of respiratory substrates (food, O_2) from the outside to the mitochondria
3. Temperature & metabolism; Q10s & Boltzmann-Arrhenius
4. Metabolism explains and underpins some profound scaling patterns in ecology, inc. community ecology, such as size spectra.

Energetic –equivalence rule

Population density/abundance scales $\propto M^{-3/4}$

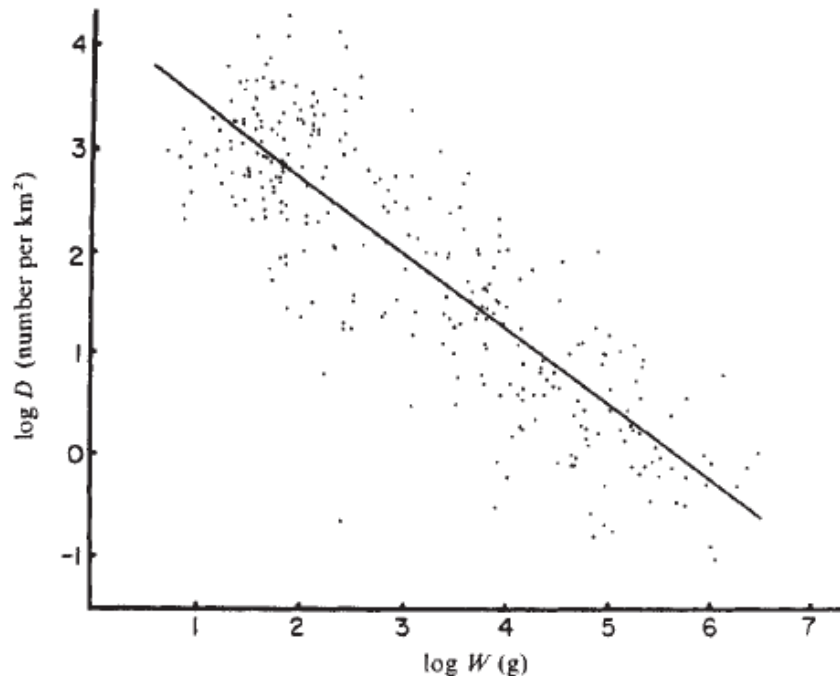
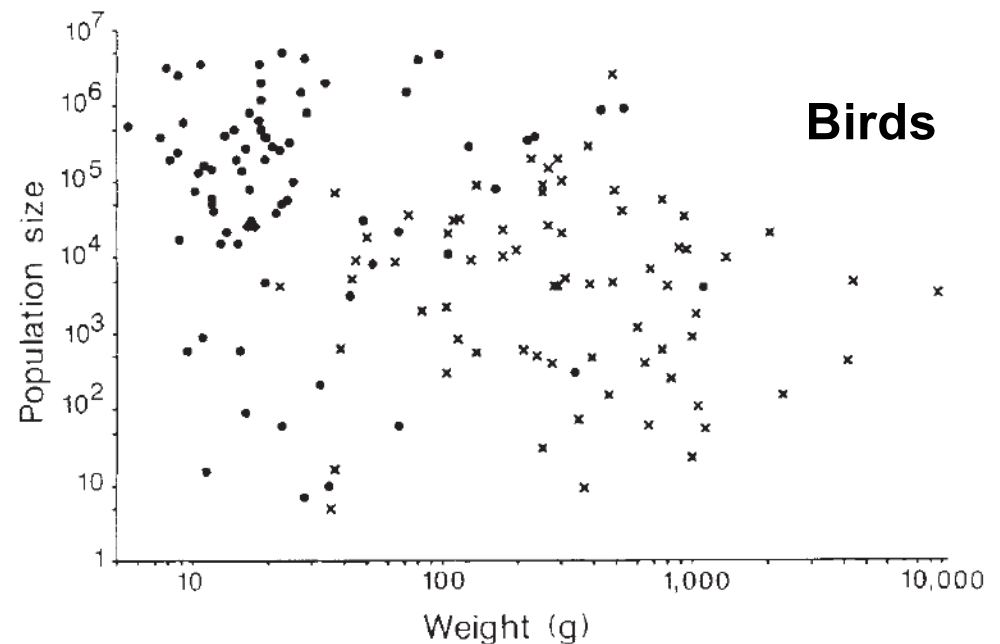


Fig. 1 Population density (D) compared with the mean adult body mass (W) for 307 mammal primary consumers; each point represents one species. Density values for each species are the mean of the means from each locality from which data were reported for the particular species. (Data are from the literature for the years 1950–79, derived from 115 journals and numerous books, ~650 references in all.) The line represents the least-squares regression line, $\log D = -0.75 (\log W) + 4.23$; $r = -0.86$, standard error of the slope = 0.026.



Damuth, J. (1981). Population density and body size in mammals. *Nature* 290, 699-700.

Nee, S., A.F. Read, J.J.D. Greenwood & P.H. Harvey. 1991. The relationship between abundance and body size in British birds. *Nature* 351: 312-313.

Population growth rate, r_{\max} , scales with $M^{-1/4}$

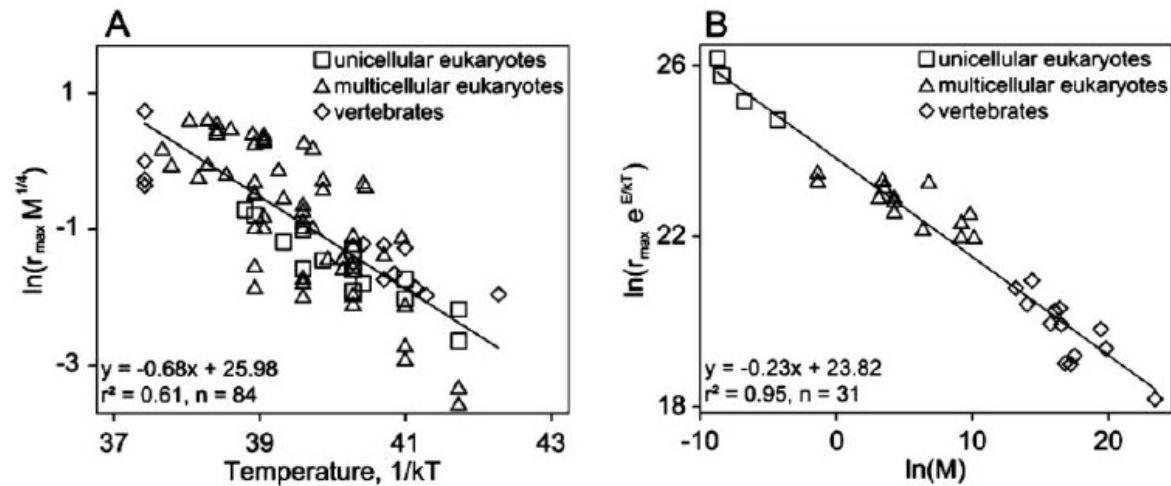
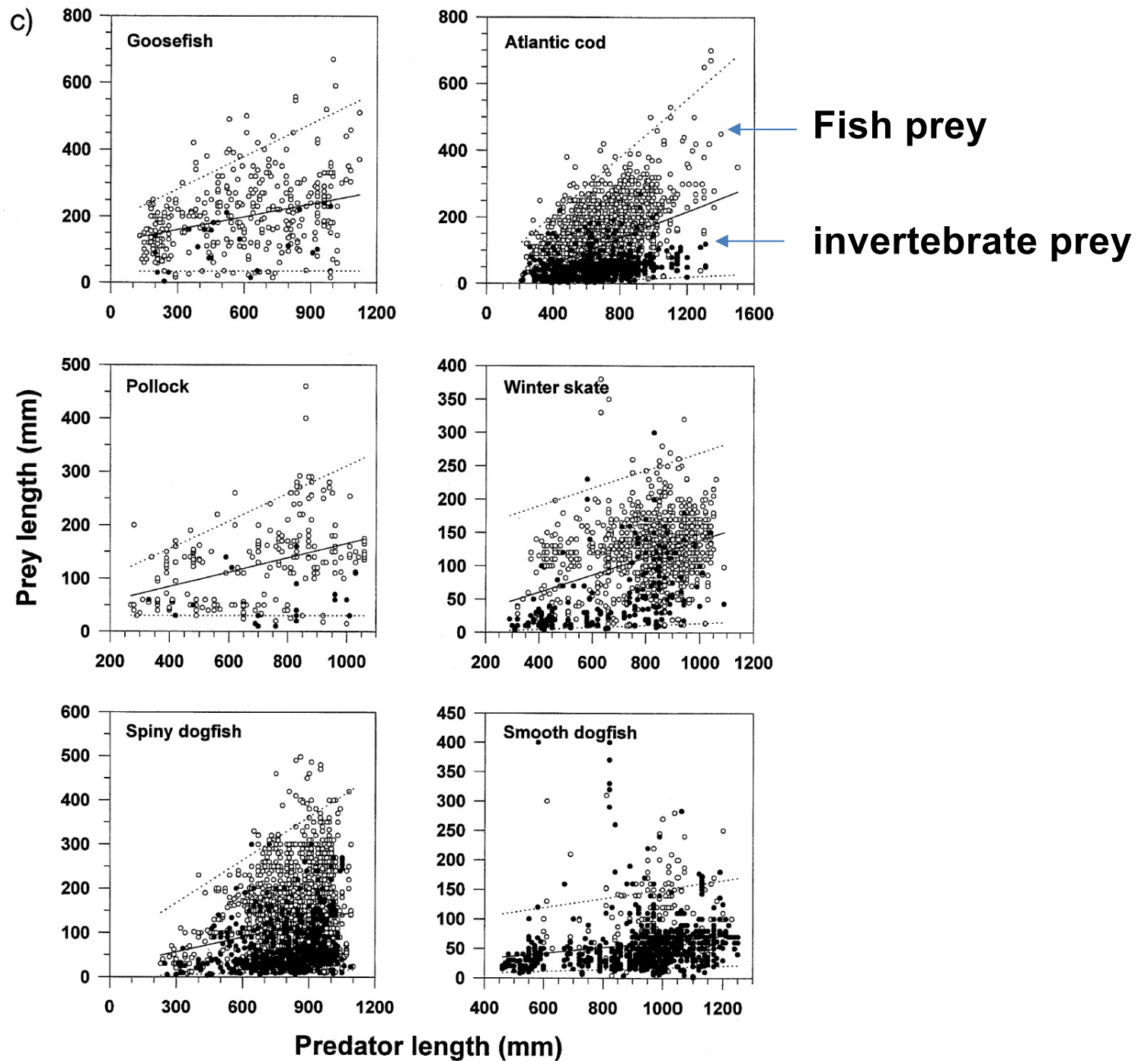


Figure 4: A, Relationship of mass-corrected exponential population growth, r_{\max} (individuals/[individual \times day]) $\times M^{1/4}$ (fresh weight, $\mu\text{g}^{1/4}$), to inverse temperature, T (1/K), for all organisms in figure 2. There is significant overlap among the data, and a single line is fit through the data. B, Relationship of temperature-corrected exponential population growth, $r_{\max} e^{E/kT}$ (individuals/[individual \times day]), to body mass, M (μg), for all organisms in figure 2. E was chosen to be 0.63 eV on the basis of an ANOVA, and each point represents the average of the logarithm of temperature-corrected r_{\max} for each species. The line was then fit using Type I linear regression. All of the data are well fit by this single straight line.

Savage, V. M., Gillooly, J. F., Brown, J. H., West, G. B., and Charnov, E. L. (2004). Effects of body size and temperature on population growth. *American Naturalist* 163, 429-441.



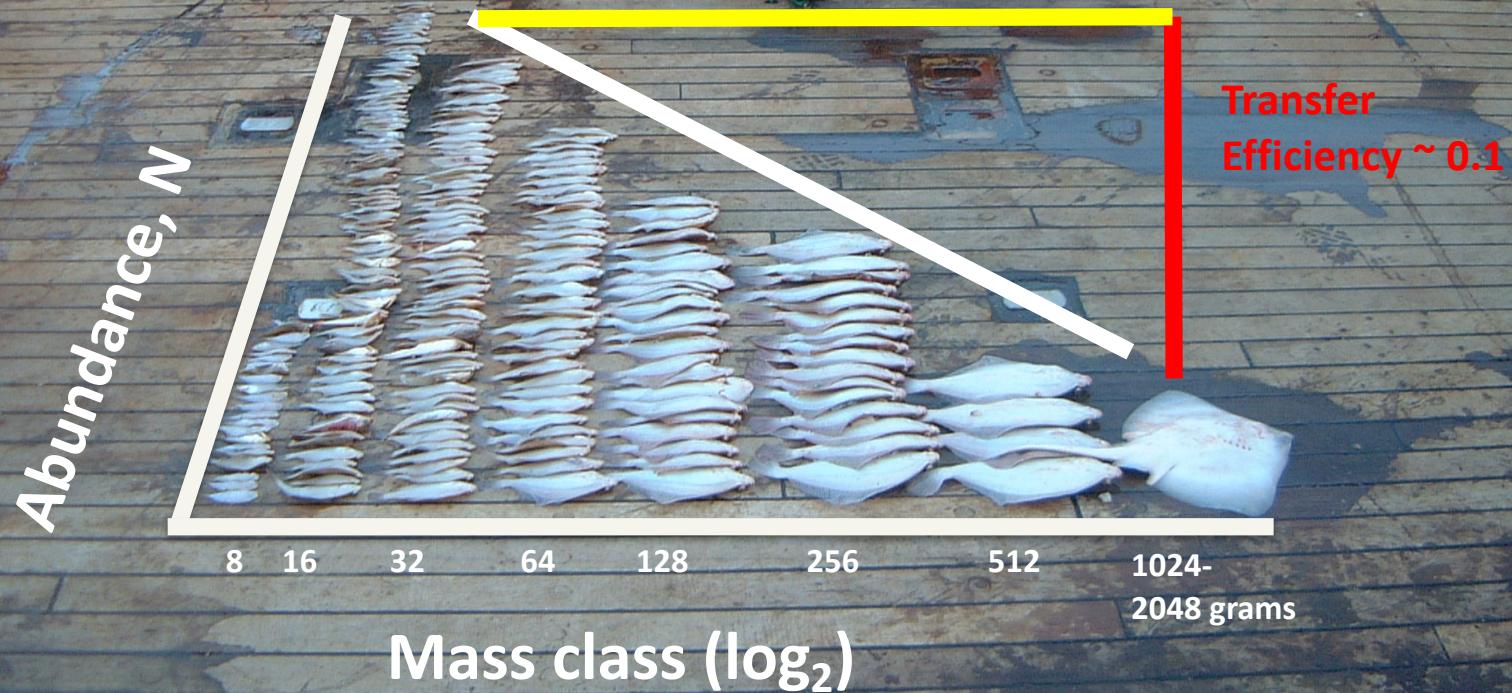
Scharf FS, Juanes F and Rountree RA. (2000) Predator-prey size relationships of marine fish predators: interspecific variation and the effects of ontogeny and body size on niche breadth. *Marine Ecology Progress Series* 208, 229-248.

Size-based view of community ecology, not yet well covered in terrestrial textbooks



$$N = aM^{-3/4} \times M^{\log(TE)/\log(PPMR)}$$

Predator-prey mass ratio ~ 0.1 to 1000



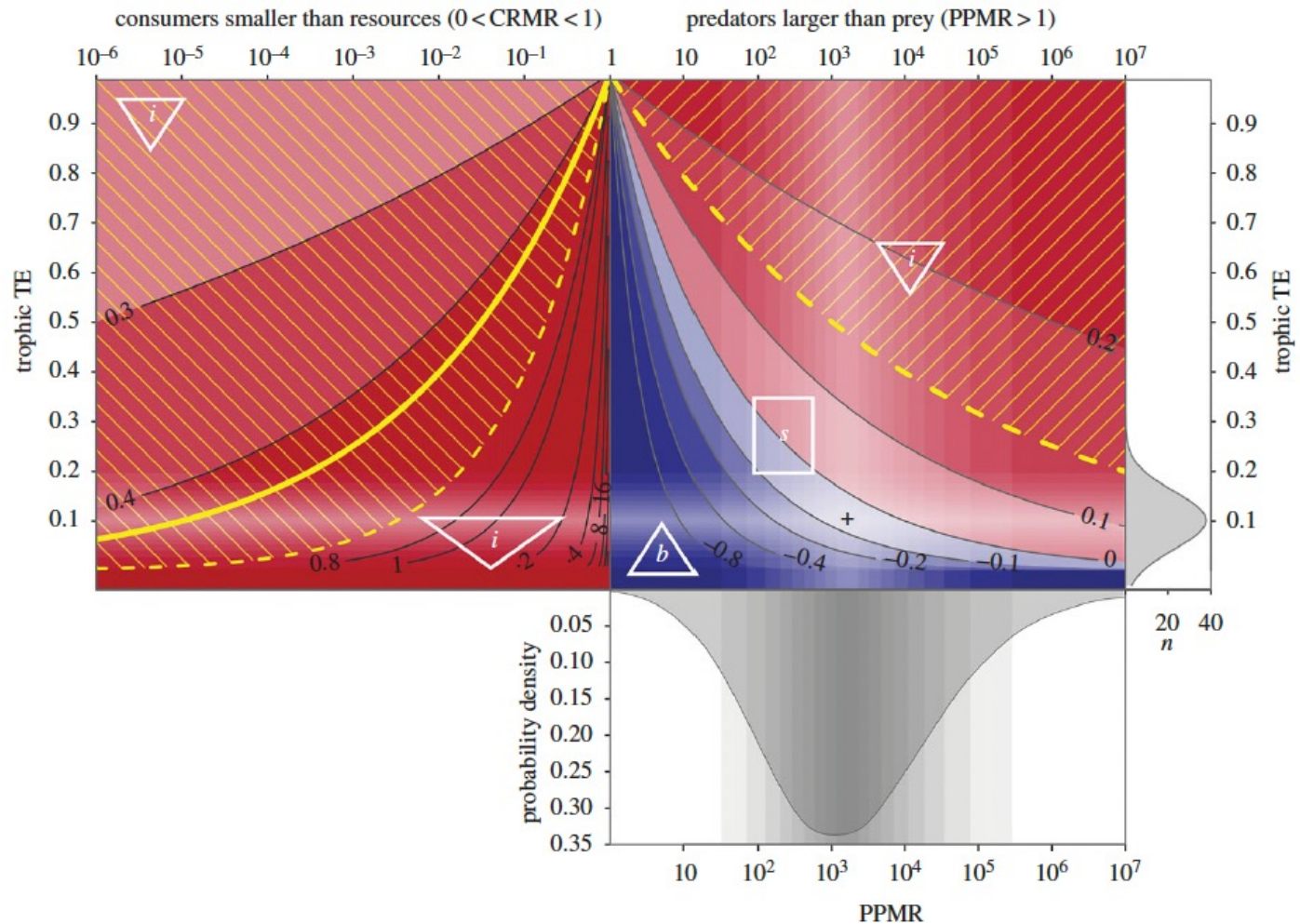


Figure 2. Expected biomass spectrum slopes (contours and red/blue shading in top panels) resulting from varying combinations of mean community PPMR and TE, shown with reference to the probability density distribution of estimated PPMR for the reef fish community of Haida Gwaii (bottom panel). The top right panel shows scenarios with predators larger than prey ($\text{PPMR} > 1$); top left panel shows scenarios with consumers smaller than resources ($0 < \text{CRMR} < 1$). Positive slopes (red area) correspond to IBPs (represented by triangles labelled i), while negative slopes (blue area) correspond to bottom-heavy pyramids (triangle labelled b) and zero slopes imply stacks/columns (rectangle labelled s). Yellow shading lines indicate the range of slopes corresponding to the 95% confidence bounds around the empirically estimated biomass spectrum slope of 0.45 (solid yellow line). Right vertical axis shows TEs derived from marine food web models ($n = 48$, mean = 0.101, s.d. = 0.058; [13]). Shaded bands represent 5% quantile increments between 5% and 95% for TE and PPMR, and the black crosshair indicates the highest probability for both distributions (PPMR = 1650, TE = 0.101).

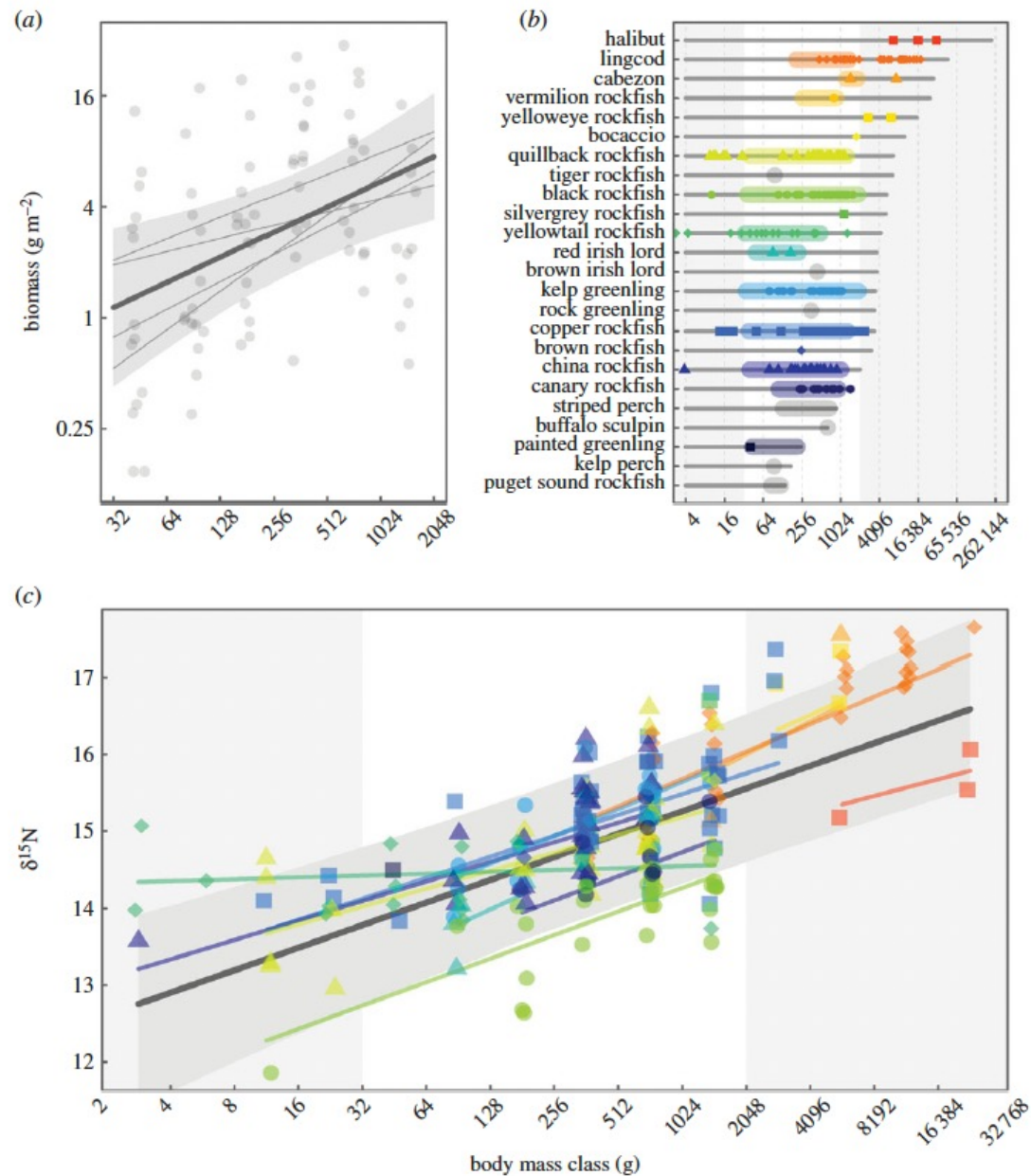


Figure 1. (a) The biomass spectrum from visual surveys; (b) size ranges observed for individual species in visual surveys (coloured shaded regions) and sampled for isotope analysis (points) relative to l_{max} (from FishBase, grey bars); and (c) the relationship between $\delta^{15}\text{N}$, a proxy for trophic position, and body size for the kelp forest fish community of Haida Gwaii British Columbia, Canada. Dark grey lines in panels (a,c) represent the mean fit for each model (across locations for (a) and across both locations and species for (c)), and grey bands indicate 95% confidence intervals in (a) and 95% credible intervals in (c) about the mean fits. Light grey lines in (a) and coloured lines in (c) represent random effect fits for location and species, respectively. Colours/shapes of points are used to distinguish among species and are consistent between panels (b) and (c), with species that were observed on transects but not sampled for isotope analysis in grey in panel (b). Grey shaded regions in (b,c) indicate body sizes outside the range included in (a).

Ocean ecosystems before humans

Box 3. The world before humans: measuring impacts and estimating baselines

The loss of large-bodied predators, rise of mesopredators, and trophic cascades are a pervasive legacy of human activities in both terrestrial and marine ecosystems, recently termed 'trophic downgrading' [53]. Management objectives are hard to define without an understanding of what once was, and what has been lost. However, because hunting and overexploitation began long before scientific data collection, appropriate baselines against which to compare modern community structure are often unavailable [74,75]. Fortunately, size spectrum theory provides a unique method of predicting the structure of ecosystems before the impact of humans.

Previous attempts to estimate how ecosystems looked before humans led to surveys of animal biomass at remote locations. These studies recorded high biomasses of large-bodied predators on relatively pristine reefs in the Pacific Ocean [11] and Mediterranean Sea [31]. The authors concluded that inverted biomass pyramids (where large predators account for the majority of the standing biomass) may represent the baseline ecosystem state for nearshore marine ecosystems, and suggested that differences in turnover rate between small and large fish account for this pattern. Although it is certain that humans have caused a significant depletion of large-bodied predators across the oceans of the world, size-based constraints on trophic pyramids (see Figure 2 in main text) show that inverted pyramids are unlikely. Instead, these apparently inverted pyramids likely result from inflated abundance estimates [76–78] and/or from the aggregation of highly mobile predators that feed and assimilate energy from pelagic sources beyond the local reef ecosystem.

Ecosystem baselines, under current climate conditions, have been estimated for the heavily exploited North Sea, and for the oceans of the world using the size spectrum approach. In the North Sea, the ecosystem baseline size spectra were markedly less steep than the observed biomass-at-size, suggesting the largest size classes had been reduced by up to and over 99% [27]. The power of ecological pyramids for communicating ecosystem structure can be shown by presenting the North Sea size spectra as pyramids (Figure 1). This shows that, although the exploited community was characterized by a very bottom-heavy biomass pyramid, the baseline expectation approached a biomass 'column' with relatively high biomass expected in large size classes. Extrapolating beyond the range of body sizes sampled also illustrates how the pyramid representation can be useful for visualising release in smaller size-classes (Figure 1).

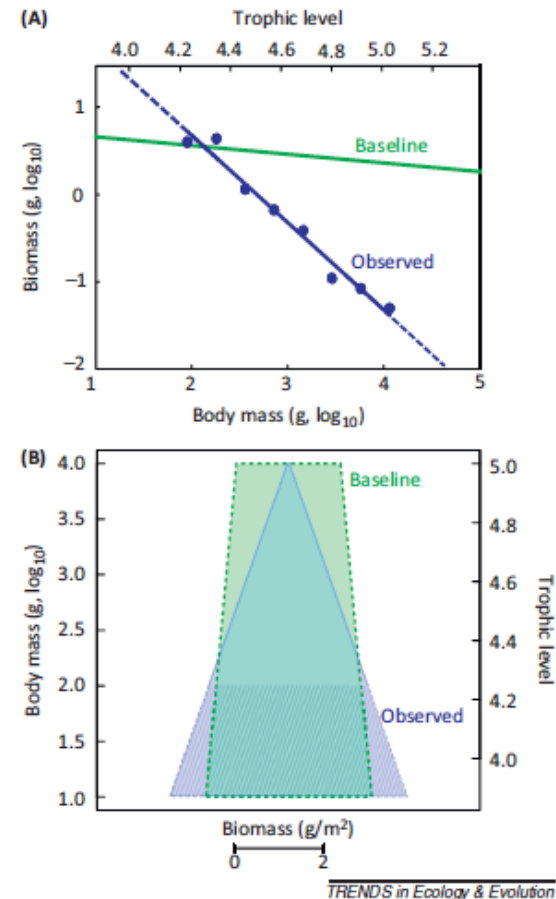


Figure 1. Re-expressing size spectra as biomass pyramids to understand baselines and community-scale impacts. **(A)** The observed (blue line and points) versus predicted baseline (green line) size spectra for the North Sea pelagic fish community can be re-expressed as biomass pyramids **(B)**, highlighting the depletion of large-bodied community members. Extrapolating past the sampled range of body sizes (striped blue region) also illustrates how pyramids can convey release in small body sizes. Adapted from [27] (A).

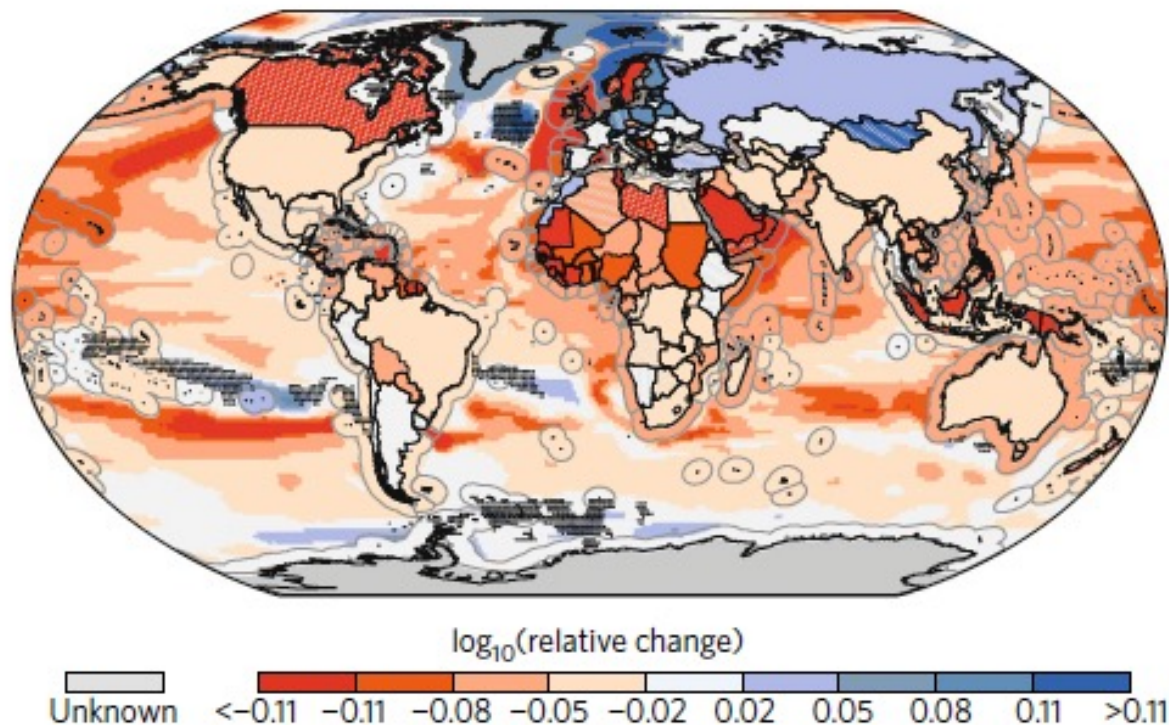


Fig. 4 | Multi-model ensemble climate change projections for potential production of marine fisheries and agriculture sectors. Projected relative changes in potential crop (maize, wheat, rice and soy combined) and fish production from Inter-Sectoral Impact Model Intercomparison Project (ISI-MIP) and Coupled Model Intercomparison Project Phase 5 (CMIP5) ensemble outputs^{92,116}. Crops are from the published agriculture model intercomparison project (AgMIP) for model ensemble outputs based on seven crop models and seven general circulation models⁸⁴. Predicted mean relative changes for total marine fish consumer biomass from the fisheries and marine model intercomparison project (FISH-MIP) model ensemble consisting of four marine ecosystem models^{82,85,87,95} forced by two Earth system models without fishing impacts. Stippling indicates model disagreement for over 50% of the models. Results are shown for RCP6.0 scenario (2050 relative to 2010) but see Supplementary Fig. 1 for comparison with other RCPs.

Four things you need to know about metabolism and community ecology

1. (Field) metabolic rates scale in a fairly predictable manner with body size, $b \sim 0.8 \sim 3/4$, due to architecture of vascular network that supplies oxygen & nutrients (West, Brown, Enquist, WBE)
2. Organismal metabolic rates are not as high as they could be, especially for larger animals. Metabolic rate is limited by the network-limiting rate of flow of respiratory substrates (food, O_2) from the outside to the mitochondria
3. Temperature & metabolism; Q_{10} s & Boltzmann-Arrhenius
4. Metabolism explains and underpins some profound scaling patterns in ecology, inc. community ecology, such as size spectra

Readings

- Bigman, J. S., M'Gonigle, L., Wegner, N. C. & Dulvy, N. K. (2021). Respiratory capacity is twice as important as temperature in driving patterns of metabolic rate across the vertebrate tree of life. *Science Advances*, 7, eabe5163.
- Brose, U., Williams, R. J., and Martinez, N. D. (2006). Allometric scaling enhances stability in complex food webs. *Ecology Letters* **9**, 1228-1236.
- Brown, J. H., Gillooly, J. F., Allen, A. P., Savage, V. M., and West, G. B. (2004). Toward a metabolic theory of ecology. *Ecology* **85**, 1771-1789.
- Brown, J. H., Gillooly, J. F., Allen, A. P., Savage, V. M., and West, G. B. (2004). Toward a metabolic theory of ecology. *Ecology* **85**, 1771-1789.**
- Brown, M. F., Gratton, T. P., and Stuart, J. A. (2007). Metabolic rate does not scale with body mass in cultured mammalian cells 10.1152/ajpregu.00568.2006. *Am J Physiol Regul Integr Comp Physiol*, 00568.2006.
- Charnov, E. L. (1993). 'Life history invariants.' (Oxford University Press: Oxford)
- Dulvy, N.K. & Forrest, R.E. (2009). Life histories, population dynamics, and extinction risks in chondrichthyans. In *Sharks and Their Relatives II: Biodiversity, Adaptive Physiology, and Conservation* (eds J.C. Carrier, J.A. Musick & M.R. Heithaus), pp. 635-676. CRC Press.
- Jennings, S., and Mackinson, S. (2003). Abundance-body mass relationships in size-structured food webs. *Ecology Letters* **6**, 971-974.
- Jennings, S., and Blanchard, J. L. (2004). Fish abundance with no fishing: predictions based on macroecological theory. *Journal of Animal Ecology* **73**, 632-642.
- Jennings, S. (2005). Size-based analyses of aquatic food webs. In 'Aquatic food webs: an ecosystem approach'. (Eds A Belgrano, UM Scharler, J Dunne et al. RE Ulanowicz). (Oxford University Press: Oxford)
- Jennings, S., and Dulvy, N. K. (2008). Beverton and Holt's insights into life history theory: influence, application and future use. In 'Advances in fisheries Science: 50 years on from Beverton and Holt'. (Eds AI Payne, AJR Cotteret et al. ECE Potter). (Blackwell Publishing: Oxford)
- Jetz, W., Carbone, C., Fulford, J., and Brown, J. H. (2004). The scaling of animal space use. *Science* **306**, 266-268.
- Savage, V. M., Gillooly, J. F., Brown, J. H., West, G. B., and Charnov, E. L. (2004). Effects of body size and temperature on population growth. *American Naturalist* **163**, 429-441.
- West, G. B., Brown, J. H., and Enquist, B. J. (1997). A general model for the origin of allometric scaling laws in biology. *Science* **276**, 122-126.
- West, G. B., Brown, J. H., and Enquist, B. J. (1999). The fourth dimension of life: Fractal geometry and allometric scaling of organisms. *Science* **284**, 1677-1679.
- West, G. B., and Brown, J. H. (2004). Life's universal scaling laws. *Physics Today* **57**, 36-42.**
- West, G. B., Woodruff, W. H., and Brown, J. H. (2002). Allometric Scaling of Metabolic Rate from Molecules and Mitochondria to Cells and Mammals. *Proceedings Of the National Academy Of Sciences Of the United States Of America* **99**, 2473-2478.

Additional reading

- Darling ES, Alvarez-Filip L, Oliver TA, McClanahan TR, Côté IM. 2012. Evaluating life-history strategies of reef corals from species traits. *Ecology Letters* **15**: 1378-1386.
- Juan-Jordá MJ, Mosqueira I, Freire J, Dulvy NK. 2013. Life in 3-D: life history strategies of tunas, bonitos and mackerels. *Reviews in Fish Biology and Fisheries* **23**: 135-155.
- Pauly D. 1981. The relationships between gill surface area and growth performance in fish: a generalisation of von Bertalanffy's theory of growth. *Meeresforschung* 28: 251-282.
- Pauly, D. & Cheung, W. W. (2018). On confusing cause and effect in the oxygen limitation of fish. *Global change biology*, 24, e743-e744.
- Pauly, D. (2021). The gill-oxygen limitation theory (GOLT) and its critics. *Science Advances*, 7, eabc6050. 10.1126/sciadv.abc6050
- Trebilco, R., Dulvy, N. K., Anderson, S. C. & Salomon, A. K. (2016). The paradox of inverted biomass pyramids in kelp forest fish communities. *Proceedings of the Royal Society B-Biological Sciences*, 283, 20160816. 10.1098/rspb.2016.0816